[8]L. G. Van Uitert and L. F. Johnson, J. Chem. Phys. 44, 3514 (1966).
[9]W. B. Gandrud and H. W. Moos, J. Chem. Phys. 49, 2170 (1968).
[10]R. C. Powell and R. G. Kepler, Phys. Rev. Letters 22, 636 (1969); 22, 1232 (1969).
[11]G. F. Imbusch, Phys. Rev. 153, 326 (1967); R. J. Birgeneau, J. Chem. Phys. 50, 4282 (1969).
[12]H. Nishimura, M. Tanaka, and M. Tomura, J. Phys. Soc. Japan 28, 128 (1970).
[13]M. Yokota and O. Tanimoto, J. Phys. Soc. Japan 22, 779 (1967).
[14]A similar physical situation and three limiting cases occur in the decay of nuclear magnetization by spin diffusion to fast-relaxing paramagnetic impurities [see W. E. Blumberg, Phys. Rev. 119, 79 (1960)].
[15]An interesting case arises if all donors are initially excited since then there is no spatial gradient of excitation and hence no diffusion is possible.
[16]More generally D is a symmetric second-rank tensor. For cubic single crystals or polycrystals and powders, D reduces to a scalar.
[17]See J. I. Kaplan, Phys. Rev. B 3, 604 (1971), and references cited therein.
[18]P. G. de Gennes, J. Phys. Chem. Solids 7, 345 (1958).
[19]M. J. Weber, E. J. Sharp, and J. E. Miller, J. Phys. Chem. Solids (to be published).
[20]E. J. Sharp, J. E. Miller, and M. J. Weber, Phys. Letters 30A, 142 (1969).
[21]L. A. Riseberg and H. W. Moos, Phys. Rev. 174, 429 (1968), and references cited therein.
[22]This is particularly evident from a semilogarithmic plot of the temperature dependence of the lifetime (see Fig. 5 of Ref. 19).
[23]A. D. Pearson, G. E. Peterson, and W. R. Northover, J. Appl. Phys. 37, 729 (1966).
[24]See, for example, Ref. 23; A. D. Pearson and G. E. Peterson, Appl. Phys. Letters 8, 210 (1966); L. G. Van Uitert, E. F. Dearborn, and H. M. Marcos, *ibid.* 9, 255 (1966).

PHYSICAL REVIEW B VOLUME 4, NUMBER 9 1 NOVEMBER 1971

Ion Energy Distributions in Field-Ion Microscopy

A. A. Lucas*
Surface Physics Division, European Space Research Organization, Noordwijk, Holland
(Received 9 April 1971)

Two currently proposed theories, resonance tunneling and surface-plasmon creation, are critically compared for the interpretation of the energy distributions of field-emitted ions measured by Jason. The properties of the spacings and intensities of the peaks of the observed oscillatory energy distribution curves are explicable in terms of an ion–surface-plasmon inelastic scattering mechanism. Some of the most important features are incompatible with the resonance tunneling effect: (i) The spacings are relatively insensitive to the chemical nature and to the pressure of the imaging gas as well as to the tip crystal face used as ion source; (ii) different metal tips, i.e., W, Pt, and Mo, produce the same peak spacings; (iii) the peak intensities strongly depend on field strength. A detailed theoretical study of a model ion-plasmon interaction Hamiltonian shows that, as a result of the strong dependence of peak spacings and intensities on field strength, field-ion emission could provide a new experimental method for investigating selectively surface collective excitations of metals. The ion-plasmon scattering effects also have important consequences for the energy distributions of ions in field desorption or evaporation and place a limitation on the mass resolution of the atom-probe microscope.

I. INTRODUCTION

This paper is concerned with the description of energy exchange processes between the ions and the electronic plasma modes at the metal tip in field-ion microscopy.

Energy distributions of field-emitted ions have been measured by Jason[1] over the range of fields normally used for the microscope operating in the imaging mode. Similar, though statistically less saturated, distributions have been obtained[2,3] by mass-spectrometry analysis of field-evaporated ions, i.e., in the "atom-probe" configuration. In Jason's experiments, the energy distributions show well-resolved oscillatory structure which has been attributed[1,4] to the resonant tunneling of electrons from the imaging gas atoms to the metal tip during the ionization process. In the atom-probe measurements, an assumed mass resolution of less than 1% has led to an interpretation of some of the broad mass spectra in terms of the formation of metastable compound ion molecules[2,3] due to the interaction between the metal-tip atoms and the imaging or residual gases.

In the present paper, it is proposed that multiple excitations of surface plasmons in the metal tip occur together with associated discrete energy losses of the imaging gas ions. It will be shown that such a process may constitute a necessary and sufficient mechanism for the origin of the struc-

TABLE I. Inventory of some observations in Jason's experiment (Ref. 1) which are important for the critical comparison of the two proposed theories of ion energy distributions in field-ion microscopy. The observations marked K.O. are at variance with the predictions of resonance tunneling theory. The second column gives the location in Jason's paper (Ref. 1) where the observation is reported. For details, see text.

Observations	Ref. 1	Resonance tunneling (Refs. 1, 4)	Plasmon creation (Ref. 5)
Peak spacings			
1. Essentially constant spacing	Fig. 9	O.K.	$\hbar\omega_s$
2. Independent of imaging gas (H_2, Ne)	Fig. 5(a)	K.O.	$\hbar\omega_s$
3. No isotope effect	p. 271	O.K.	$\hbar\omega_s$
4. No temperature effect (T)	p. 271	O.K.	$\hbar\omega_s$
5. No pressure effect (P)	p. 271	K.O.	$\hbar\omega_s$
6. No tip radius effect (R)	p. 271	O.K.	$\hbar\omega_s$
7. No crystal face effect (C)	p. 274	K.O.	$\hbar\omega_s$
8. Same peak spacings for W, Pt, Mo tips	p. 274	K.O.	$\hbar\omega_s$
9. Decrease of spacing with decreasing field strength	Fig. 8	O.K.	$\hbar\omega_s(k)$
10. Decrease of spacing with increasing distance from parent peak	Fig. 8	O.K.	$\hbar\omega_s(k)$
Peak intensities			
11. Damped distrib. at low fields	Fig. 4	K.O.	Poisson distrib.
12. I_1/I_0 increases with field; crossing of first three loss curves	Fig. 10	K.O.	Poisson distrib.
13. At high field: decay of parent peak and broad distrib.	p. 276	K.O.	Poisson distrib.
14. Weaker structure with Ne instead of H_2	Fig. 5(b)	K.O.	Poisson distrib.

tures in both kinds of energy distributions.[5]

Table I is a compilation of some of the numerous features observed in the energy spectra discussed by Jason.[1] We refer to Refs. 1 and 4 for the detailed arguments put forward in support of the resonance tunneling theory. The main point that needs to be emphasized here is that the predictions of the resonance theory, as regards the structure of the resonance peaks, depend rather critically on the detailed shape of the tunneling barrier. However, observations 2, 5, 7, and 8 in Table I clearly show that the oscillatory distributions remain relatively insensitive to the precise nature of both the surface and atomic potentials. Also, the resonance tunneling mechanism appears to be incompatible with the observed strong dependence of the relative peak intensities on field strength (Table I, observations 11–14).

To understand the proposed plasmon excitation mechanism, first recall that the Coulomb field of a classical charged particle traveling in the vicinity of a metal surface is partially shielded by the field of an image charge which is set up in the metal. The image charge builds up as a result of the average dynamical response of surface plasmons in the metal tip to the long-range field of the external charged particle.[6] Bulk plasmons or individual quasiparticles of the bulk do not respond significantly to charges traveling at distances from the surface larger than the lattice spacing. It will be shown that the relevant coupling parameter for the ion–surface-plasmon dynamical interaction is provided, as expected, by the ratio of the image charge potential energy and the surface-plasmon energy quantum

$$g = \frac{Z^2e^2/4z}{\hbar\omega_s} \quad , \tag{1}$$

where Ze is the ion charge and z is the distance between the ion and the surface. Thus, using a typical plasmon frequency ($\hbar\omega_s \simeq 10$ eV) and $Z = 1$, the coupling "constant" is larger than, say, 0.01 for values of z up to several tens of angstroms. For quadruply ionized species, one finds $g \geq 10^{-2}$ up to $z \leq 500$ Å.

Another factor of importance in controlling the ion-plasmon coupling is the total energy conservation for the combined ion-metal system. Discrete amounts of energy $n\hbar\omega_s$ can be lost by the accelerating ion due to the coupling with the surface-plasmon field, the loss process beginning as soon as the ion kinetic energy has been increased above the threshold energy $\hbar\omega_s$. In the large fields (several V/Å) used in the ion microscope, the minimum energy required to excite a surface plasmon is reached within a few angstroms from the tip surface. The scattered ions will then arrive at the screen with corresponding discrete energy deficits and enter the spectrometer, giving rise to an energy distribution oscillating with period $\hbar\omega_s$. Fig. 1 illustrates the phenomenon in an energy-time phase space.

The above interpretation in terms of multiple losses of surface-plasmon quanta is not contradicted by any of the experimental data listed in Table I.

A first critical test of the theory concerns the actual value of the observed spacing, i.e., $\hbar\omega_s \simeq 7$ eV for W, Pt, and Mo tips at low fields.[1] Does one observe a surface plasmon around this energy for these materials in independent measurements? A positive answer is provided by recent experimental studies of optical properties of transition metals.[7,8] Current measurements in this laboratory[9] using electron energy loss spectroscopy of Pt, W, and Mo appear to endorse these results. The energy loss function $\mathrm{Im}\epsilon^{-1}(\omega)$ obtained from these measurements shows a relatively well-defined peak at about $\hbar\omega_B \simeq 10$ eV for Pt, W, Mo, Ru, and Re, suggesting the likely existence of a long-wavelength *bulk* collective excitation around that energy in all these metals. The corresponding surface plasmon will have energy at approximately $\hbar\omega_s = \hbar\omega_B/\sqrt{2} \simeq 7$ eV, in agreement with the observed spacing at low field.[1]

Second, one may ask if the plasmon creation

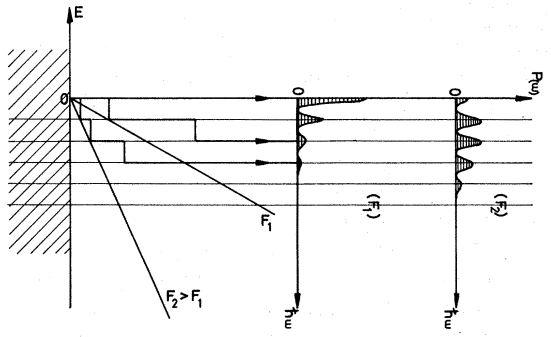

FIG. 1. Representation, in an energy-time phase space, of possible scattering processes contributing to the generation of a loss spectrum (vertical shaded area). The equidistant horizontal lines represent the quantized surface-plasmon energy states of the metal tip (shaded area). At higher field strength (F_2), the excitation of the surface plasmons occurs with a higher probability due to the smaller distances from the tip at which the ions can be scattered. A peak in the loss spectrum is proportional to the product of the probabilities of consecutive scattering events, the net ion energy loss effectively moving down the energy ladder with increasing time.

mechanism can account for the observed decrease of the peak spacings when (i) one decreases the field strength (Table I, observation 9) or (ii) when one examines the higher-order energy deficits for a given field strength (Table I, observation 10). It will be argued below that both effects are explicable in term of the dispersion relation $\omega_s(k)$ of surface plasmons. This remarkable result suggests a new and unique method of selectively measuring the excitation spectrum of only surface plasmons over a substantial portion of k space.

Third, it will be shown that the dependence of the relative peak intensities on field strength (Table I, observations 11 – 14) is entirely consistent with the present interpretation of the distributions being energy loss spectra similar to those observed in electron energy loss spectroscopy.[10–12]

Finally, it will be shown that in field desorption, evaporated ions could be scattered by the surface-plasmon field sufficiently strongly to arrive at the spectrometer with energies almost randomly distributed within a range several hundreds of eV wide.

In Sec. II, a model Hamiltonian for the system ion-plasmons is introduced. Section III contains details of the calculation of the loss spectrum in a semiclassical approximation. In Secs. IV–VI, the results and predictions of the present theory are presented. Section VII summarizes the conclusions of this work.

II. MODEL FOR PLASMON-ION INTERACTION

The Hamiltonian for the interacting plasmon-ion system is taken to be

$$H = H_p + H_i + V_{ip} , \tag{2}$$

$$H_p = A \int d\vec{k}\, \hbar\omega_k \,(\alpha_k^\dagger \alpha_k + \tfrac{1}{2}) , \tag{3}$$

$$H_i = p_\rho^2/2M + p_z^2/2M - ZeFz , \tag{4}$$

$$V_{ip} = A \int d\vec{k}\, C(\vec{k})\, e^{-i\vec{k}\cdot\rho - kz}\, (\alpha_k^\dagger + \alpha_k)\, \theta(z - z_0) . \tag{5}$$

H_p describes the surface plasmons of a semi-infinite homogeneous free compensated electron gas. $\vec{k}$ is a two-dimensional wave vector parallel to the surface and A is a unit area of the surface. H_i is the Hamiltonian of the ion with coordinates $\vec{r} = (\vec{\rho}, z)$ parallel and normal to the surface, respectively, and F is the applied field. V_{ip} is the second-quantized form of the plasmon-ion interaction[10–12] in which

$$C(k) = (\hbar Z^2 e^2 \omega_p^2 / 8\pi A\, k\omega_k)^{1/2} , \tag{6}$$

where $\omega_p = [4\pi(ne^2/m)_{\text{eff}}]^{1/2}$ is an effective bulk plasma frequency for the collective modes under consideration. θ is the step function

$$\begin{aligned} \theta(z - z_0) &= 0 \ \text{ if } z < z_0 \\ &= 1 \ \text{ if } z > z_0 , \end{aligned} \tag{7}$$

where z_0 is the distance from the tip surface at which the ion is created. z_0 equals the critical distance (z_c = const/field) in field emission or is approximately zero in field evaporation.[13]

That Eq. (5) gives the correct analytical form of the metal-ion interaction can be readily understood by recalling the following: (a) In any linear response theory, the interaction will be linear in the amplitudes of the electronic polarization fields and hence in the field operators α_k.

(b) Because one is considering a planar surface geometry, the interaction should be translationally invariant for displacements parallel to the surface (factor $e^{-i\vec{k}\cdot\vec{\rho}}$).

(c) The Laplace equation $\Delta V = 0$ applied to a free polarization potential of the form $V = \int d\vec{k}\; V_k(z) e^{-i\vec{k}\cdot\vec{\rho}}$ reduces to

$$\frac{\partial^2 V_k(z)}{\partial z^2} - k^2 V_k(z) = 0 \tag{8}$$

and therefore implies that the free surface fields must decay exponentially away from the surface (factor e^{-kz}). The correctness of the coupling "constant" $C(k)$ can be checked by considering the case of a static point charge for which $\vec{r} = (\vec{\rho}, z)$ is not an operator but a constant. For this case, one should recover, from Eq. (5), the classical image charge potential energy. Taking $\vec{\rho} = 0$, the Hamiltonian (2) reduces to

$$H = A \int d\vec{k}\, [\hbar\omega_k(\alpha_k^\dagger \alpha_k + \tfrac{1}{2}) + C(k) e^{-kz}(\alpha_k^\dagger + \alpha_k)] - ZeFz \tag{9}$$

and is diagonalized by the translation

$$\alpha_k \equiv a_k + [C(k)/\hbar\omega_k]\, e^{-kz} \tag{10}$$

expressing the accumulation of screening imaging

charge in the metal. This gives

$$H = A\int d\vec{k}\{\hbar\omega_k(a_k^\dagger a_k + \tfrac{1}{2}) - [C^2(k)/\hbar\omega_k]\,e^{-2kz}\} - ZeFz\,. \tag{11}$$

The ground-state energy of the system is

$$E_0 = A\int d\vec{k}\,\tfrac{1}{2}\hbar\omega_k - W - ZeFz\,, \tag{12}$$

where

$$W = A\int d\vec{k}\,[C^2(k)/\hbar\omega_k]\,e^{-2kz} \tag{13}$$

is the interaction part of the ion-metal system. Substituting Eq. (6), one obtains

$$W = \tfrac{1}{4}z^2e^2\omega_p^2\int_0^{k_c} dk\,e^{-2kz}/\omega_k^2\,. \tag{14}$$

If $z \gg k_c^{-1}$, one can use the long-wavelength limit $\omega_k^2 = \frac{1}{2}\omega_p^2$ and take $k_c \to \infty$. This yields

$$W = Z^2e^2/4z\,, \tag{15}$$

which is just the classical image charge interaction energy, as it should be.

An important requirement for the validity of this model with regards to the present physical system is that the ion coordinate z should be smaller than the tip radius and bigger than the lattice constant. In fact, the interaction (5) tends to zero for both large and small z and is perfectly valid for the case of field-ion emission where z_0 is usually several angstroms. In field evaporation, and, in particular, for the atom probe, the above model is not strictly valid at very small distances from the surface since the atomic details of the surface are ignored. In spite of this, the Hamiltonian (2) is appropriate to the description of the loss processes in field evaporation as well as field emission because the existence of a kinetic-energy threshold $\hbar\omega_s$ prevents losses from occurring until the ion has moved to some distance away from the tip.

Before proceeding with the study of the Hamiltonian (2), it should be stated here that the precise analytical form of the coupling is characteristic of a high-density free-electron gas. However, although deviations from this simple form may be expected to occur when dealing with real metals, the main characteristics of the coupling, i.e., its linearity in the plasmon field operators and its rapid decay with increasing distance z, are general features of collective surface oscillations.

The problem of finding a good approximation for the eigenstates of the stationary Hamiltonian (2) poses difficulties, especially when one realizes that first-order scattering theory is inadequate in the present situation. Since the ion-plasmon interaction term (5) contains linear plasmon field operators, losses involving n plasmons (and generating the nth peak in the observed oscillatory structure) represent perturbation processes of nth order. Some of these processes are sketched in Fig. 1. One cannot resort to an *ad hoc* argument of consecutive first-order scatterings as has been invoked in electron energy loss spectroscopy[12,14] of isotropic bulk materials. The idea of consecutive losses amounts to the introduction of a mean free path between successive ion-plasmon scatterings with exchange of a single energy quantum $\hbar\omega_s$. Clearly, this notion is meaningless here since the interaction Hamiltonian has a strong z dependence.

Rather, we will formulate a semiclassical approach in which the multiple-scattering aspect of the problem will be fully included. It is assumed that the ion is traveling radially along the classical trajectory

$$\vec{\rho} = 0\,, \quad z(t) = \tfrac{1}{2}\gamma t^2 + v_0 t + z_0\,, \tag{16}$$

where $\gamma = ZeF/M$ is the constant acceleration in the homogeneous field F and v_0 is the initial, generally small, thermal velocity of the ion at the instant of its creation. In this case, the ion acts as a time-dependent perturbation for the plasmon field such that excitations occur from the initial state to some higher excited surface-plasmon state. Using energy conservation, the energy spectrum of the outgoing ions can be deduced from the asymptotic time evolution of the plasmon field.[12] The intensity of the ion energy distribution is proportional to the loss spectrum, which is defined as the probability of finding, at time $t \to \infty$, the plasmon field in any state of excitation $\hbar\omega$ above the ground state, i.e.,

$$P(\omega) = \lim_{t\to\infty}\sum_{\{n_k\}} |\langle\Psi(t)|\{n_k\}\rangle|^2\,\delta(\omega - \textstyle\sum_k n_k\omega_k)\,, \tag{17}$$

where $|\{n_k\}\rangle$ is an eigenstate of the free plasmon Hamiltonian (3) and $|\Psi(t)\rangle$ is the state vector of $H_p + V_{ip}(t)$.

As it stands, the above semiclassical approach neglects an important feature of the scattering process, i.e., the ion recoil on emission of a plasmon. A first improvement of the theory would be to use, instead of Eq. (16), the more exact classical equation of motion taking into account the classical image potential. This average attractive image force prolongs the time spent by the ion within the critical zone for plasmon generation and this tends to enhance the energy losses. An enhancement of a similar nature is expected to result from the quasidiscontinuous reductions suffered by the ion velocity on emission of one or more plasmsons. A proof of this enhancement effect will be given in Sec. IV. The probabilistic nature of plasmon generation makes it difficult, if not possible, to include these sudden recoils in a self-consistent semiclassical theory. By using the unperturbed trajectory (16), the problem can be solved exactly and, for the reasons discussed above, the solution is expected to provide a lower bound for the transition probabilities involved.

III. CALCULATIONS

To calculate $P(\omega)$ in Eq. (17), one uses $\delta(x) = (2\pi)^{-1}\int_{-\infty}^{+\infty} d\tau\, e^{ix\tau}$ to eliminate the complete set of intermediate states $|\{n_k\}\rangle$:

$$P(\omega) = \frac{1}{2\pi}\int_{-\infty}^{+\infty} e^{i\omega\tau} P(\tau)\, d\tau , \tag{18}$$

where

$$P(\tau) = \lim \langle \Psi(t) | e^{-i(H_p - E_0)\tau} | \Psi(t)\rangle \quad \text{as } t\to\infty, \tag{19}$$

and where E_0 is the ground-state energy of the plasmon field. The time correlation function (19) can then be calculated using standard canonical transformation techniques.[15] The result is

$$P(\tau) = P_0 \exp\left(A\int d\vec{k}\, \frac{|I(k)|^2}{k^2} e^{-i\omega_k\tau}\right) , \tag{20}$$

$$I(k) = C(k)\int_{-\infty}^{+\infty} dt\, e^{-i\omega_k t}\, e^{-kz(t)}\,\theta(t) . \tag{21}$$

P_0 is the normalization constant of the loss spectrum:

$$P_0 = 1/P(\tau = 0) , \tag{22}$$

so that

$$\int_{-\infty}^{+\infty} d\omega\, P(\omega) = 1 , \tag{23}$$

as it should, since the definition (17) is normalized.

Introducing Eq. (16) into Eq. (21), one obtains[16]

$$I(k) = \tfrac{1}{2}C(k)\, e^{-kz_0}\left(\frac{2\pi}{k\gamma}\right)^{1/2} \exp\left(\frac{(kv_0 + i\omega_k)^2}{2k\gamma}\right) \times \operatorname{erfc}\left(\frac{kv_0 + i\omega_k}{(2k\gamma)^{1/2}}\right) , \tag{24}$$

where erfc(x) stands for complement of the error function. At this point, one could expand the correlation function (20) in powers of the interaction function $I(k)$ and integrate Eq. (18) term by term. This generates the perturbation expansion

$$P(\omega) = P_0\left(\delta(\omega) + A\int d\vec{k}\, \frac{|I(k)|^2}{1!\,\hbar^2}\,\delta(\omega - \omega_k) + A^2\iint d\vec{k}\, d\vec{k}'\, \frac{|I(k)|^2 |I(k')|^2}{2!\,\hbar^2}\,\delta(\omega - (\omega_k + \omega_{k'})) + \cdots\right) . \tag{25}$$

The first term is the zero-loss probability and therefore P_0 gives the strength of the no-loss line. The shape of the parent peak is obtained by multiplying with this factor P_0 the ordinary energy distribution arising from the finite width of the ionization zone.[13] The second term in Eq. (25) gives the single-plasmon excitation probability and hence the intensity of the first energy loss maximum, etc. If one includes finite lifetime effects, the δ-shape lines broaden to Lorentzians with half-width equal to the cumulative damping $\Delta\omega_k + \Delta\omega_{k'} + \cdots$. Thus, the actual shape of the first deficit peak results from a multiple folding integral over (i) the shape of the parent peak, (ii) the dispersion relation ω_k, (iii) the lifetime broadening, and (iv) the resolution function of the spectrometer. Nevertheless, in spite of these complications, some useful information concerning the plasmon dispersion relation can be gained by careful studies of the loss spectrum. If the amount of dispersion involved in the multiple k integrals of Eq. (25) is not too large, then the over-all spectrum should have the shape of a Poisson distribution characteristic of loss spectra.[12] The distributions obtained by Jason[1] do exhibit this shape.

To gain more insight into the nature of the loss spectrum and, in particular, to study its dependence on field strength, we shall make the nonessential assumptions $v_0 = 0$ and $\omega_k = \omega_s$ (neglect of surface-plasmon dispersion). This permits the k integral of Eq. (20) to be done exactly. Introducing the parameter $\alpha = \omega_s/(2k_c\gamma)^{1/2}$, where k_c is the limiting wave vector for plasmons,[14] and using the reduced variables

$$u = \omega_s^2/k\gamma , \quad v = \omega_s/(2k\gamma)^{1/2} , \tag{26}$$

$P(\tau)$ is found to be

$$P(\tau) = P_0 \exp\left\{Z^2\alpha^2 \frac{\pi k_c e^2}{2\hbar\omega_s}\left[\int_{2\alpha^2}^{\infty} du\, \frac{e^{-u}}{u}\, e^{-4\alpha^2 k_c z_0/u} + \frac{8}{\pi}\int_{\alpha}^{\infty} \frac{dv}{v}\, e^{-2\alpha^2 k_c z_0/v^2} e^{-2v^2}\left(\int_0^v e^{z^2} dz\right)^2\right] e^{-i\omega_s t}\right\} . \tag{27}$$

The first integral amounts to less than the exponential integral[16] $-Ei(-2\alpha^2) = \int_{2\alpha^2}^{\infty} du\, e^{-u}/u$ and contributes negligibly to the result since, for field-ion emission, $\alpha \simeq 100$. The second term in Eq. (27) involves the Dawson integral[16]

$$D(v) = e^{-v^2}\int_0^v e^{z^2} dz , \tag{28}$$

which, for large v (here $v \gtrsim \alpha$), behaves like[16]

$$\lim_{v\gg 1} D(v) = 1/2v \quad \text{for } v \gg 1 . \tag{29}$$

Substituting Eq. (29) into Eq. (27), the remaining v integral has the elementary form $\int dv\, e^{-\alpha/v^2}/v^3$ and gives the final result

$$P(\tau) = P_0 \exp\left[(1 - e^{-2k_c z_0}) \frac{Z^2 e^2/4z_0}{\hbar\omega_s} e^{-i\omega_s \tau}\right] . \quad (30)$$

The generalization of these results to the case where there exist several independent branches $\omega_s^\mu(k)$ in the dispersion relation for surface plasmons is straightforward. For instance, if the bands are relatively flat in the k region of interest, the generalized time correlation function corresponding to Eq. (30) is

$$P(\tau) = P_0 \exp\left[\sum_\mu (1 - e^{-2k_c^\mu z_0}) \frac{Z^2 e^2/4z_0}{\hbar\omega_s^\mu} e^{-i\omega_s^\mu \tau}\right] . \quad (31)$$

This is the case for the transition metals Pt, W, Mo, Ru, Ta, and Re. In addition to the low-lying collective mode around 10 eV discussed in the Introduction, they all show a well-defined high-energy bulk plasmon ranging from 20 to 26 eV, in agreement with the expected value if five to seven electrons per atom participate in the collective mode.[8,9]

One recognizes in the functions (30) and (31) the coupling parameter g introduced in Eq. (1) and discussed in the Introduction.

The final piece of information necessary to complete this theoretical model is the relationship between critical distance z_0 and applied field F. This relation is well known[13]:

$$z_0 = C/F , \quad (32)$$

where C is related to the ionization energy I of the imaging gas and the work function Φ of the metal,

$$C \simeq (I - \Phi)/Ze . \quad (33)$$

In summary, when applying the model to a particular experiment, the following set of independent quantities is to be considered:

metal tip , $(\omega_s^\mu, k_c^\mu, \Phi)$;

imaging gas or evaporating species, (I, Z);

applied field, F.

IV. DISCUSSION OF NO-RECOIL THEORY

We illustrate the above theoretical results by considering a numerical example which is meant to describe approximately the spectrum of H_2^+ ions imaging a tungsten tip. The relevant parameters are $Z = 1$, $\hbar\omega_s = 7$ eV, $C = 10$ V (F in V/Å), and $k_c = 10^8$ cm^{-1}. The value of k_c is rather uncertain since, at present, the exact nature of the collective excitation observed at 10 eV in transition metals[7-9] is not known. Fortunately, the result (30) does not depend critically on this parameter. One finds

$$P(\tau) = P_0 \exp[0.05(1 - e^{-20/F}) F e^{-i\omega_s \tau}] . \quad (34)$$

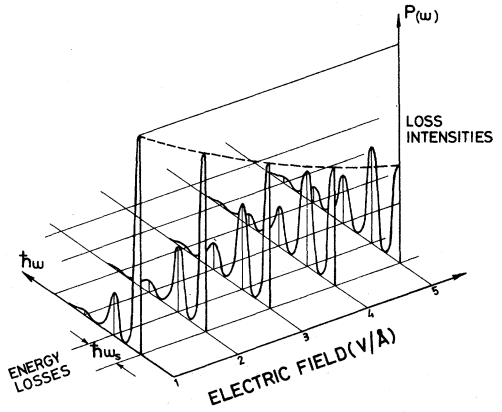

FIG. 2. Predicted energy distribution of field-emitted ions as a function of field strength. Each spectrum is normalized according to $\int_0^\infty P(\omega)\, d\omega = 1$ and satisfies the sum rule $\int_0^\infty \hbar\omega P(\omega)\, d\omega =$ classical total energy loss (Ref. 12). A damping $\Delta\omega/\omega_s \simeq 0.3$ of the surface plasmon has been introduced to allow for finite lifetime effects. The dotted exponential line in the vertical plane gives the strength of the no-loss peaks.

Expanding in powers of F, the Fourier transform (18) will again generate a Poisson-like distribution of equidistant peaks. Figure 2 is a schematic drawing of the predicted spectra for various field strengths. In this figure, the loss strength has been multiplied by a factor of 4 for clarity of the picture. The ratio between the nth peak and zero-order peak strengths is predicted to increase with increasing field,

$$I_n/I_0 = [0.05(1 - e^{-20/F}) F]^n/n! . \quad (35)$$

Physically, this field enhancement of the deficit structure is easily understood. At higher fields, both the ionization and acceleration of the ions to energies greater than the threshold $\hbar\omega_s$ take place closer to the tip surface, where the ion must travel through a denser surface-plasmon cloud. Referring to Fig. 10 of Ref. 1, which we reproduce here as Fig. 3, one can see that this correctly predicts the general trend of increasing loss probabilities with increasing fields. Two particularly convincing features are the crossing of the successive secondary peak intensities at high field and the gradual weakening of the parent peak. This is characteristic of a Poisson distribution, Eq. (35) (Table I, observations 11–13). However, the observed increase is faster than predicted by Eq. (35) and the observed plateau is not accounted for in the present model. These effects may be due to the enhancement of the loss processes resulting from the ion recoil on emission. One can actually demonstrate that such an enhancement must result when recoil is included in the theory. Referring to Fig. 4, we want to compare what can be called the "remaining" scattering

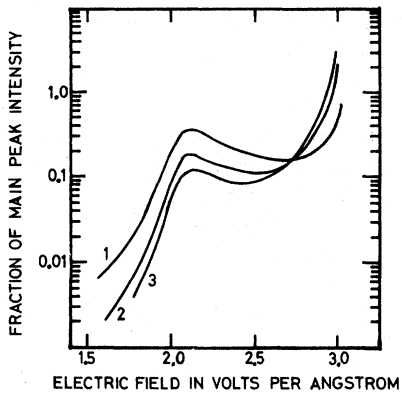

FIG. 3. Ratio of the first three deficit peak intensities to the parent peak intensity as a function of the field strength. H_2^+ ions imaging a 250-Å W tip at 20 °K. Reproduced from Fig. 10 of Ref. 1.

probabilities for an ion arriving at time t' and velocity $v' \simeq \gamma t'$ at some arbitrary distance z' without having been previously scattered (case A), and for an ion arriving at the same point after having already suffered multiple losses (case B). Using Eq. (21), the two probability amplitudes are proportional to

$$I_A(k) = C(k) \int_0^\infty dt\, e^{-i\omega_k t}\, e^{-kz(t)} \theta(t - t') , \tag{36}$$

$$I_B(k) = C(k) e^{-kz'} \int_0^\infty dt\, e^{-i\omega_k t} e^{-kz(t)} , \tag{37}$$

respectively. In Eq. (36), the θ step function cuts out the interaction for $0 < z < z'$ to eliminate scattering in this range. In Eq. (37), the origin of time has been chosen at the time of arrival of the ion at $z' = z(t')$ (with zero velocity, if the ion has been totally scattered, as in Fig. 4). Changing the integration variable in Eq. (36) from t to $\tau = t - t'$ and using the trajectory Eq. (16) (in which one can neglect the z_0 and v_0 terms for simplicity), one finds

$$z(t) = z(\tau) + z(t') + \tau v' , \tag{38}$$

and therefore

$$I_A(k) = e^{-i\omega_k t'} C(k) e^{-kz'} \int_0^\infty d\tau\, e^{-i\omega_k \tau} e^{-kz(\tau)} e^{-k\tau v'} . \tag{39}$$

Comparing this last expression with Eq. (37), one recognizes that

$$|I_A(k)| < |I_B(k)| \tag{40}$$

due to the reduction factor $e^{-k\tau v'}$, which expresses the smaller time spent by the ion in the zone of influence of the plasmon field in case A.

V. SEMIEMPIRICAL RECOIL THEORY

The above analysis suggests a semiempirical way to include recoil into the theory. The form of the factor $e^{-k\tau v'} = e^{-k\gamma\tau t'}$ affecting the no-recoil probability amplitude I_A indicates that the true total scattering probability amplitude $I_R(k)$, with recoil included, should contain an enhancement factor depending exponentially on γ and, hence, on field strength F. Physically, recoil by plasmon creation is a self-generating process since, according to Eq. (40), scattering at a given distance from the tip favors further scattering in the remaining flight of the ion. Therefore, we propose to use the phenomenological relationship

$$I_R(k) = e^{akF} I(k) , \tag{41}$$

where $I(k)$ is the no-recoil total amplitude of Eq. (24), and where a is a real positive parameter to be determined empirically. The enhancement factor also has the right k dependence and reduces to unity for $k = 0$: No enhancement should be expected for vanishing-k surface plasmons since the electric field they generate is uniform throughout space.

Neglecting the v_0 terms in Eq. (24) and using the limit[16] $\lim(\sqrt{\pi}) e^{x^2} x \operatorname{erfc}(x) = 1$ for $|x| \gg 1$ [equivalent to Eq. (29)], one obtains

$$I_R(k) = [c(k)/\omega_k]\, e^{akF - kz_0} . \tag{42}$$

From Eq. (25), the single-loss line P_1^R is now given by

$$P_1^R(\omega, F) = P_0 \frac{Z^2 e^2 \omega_s^2}{2\hbar} \int_0^{k_c} dk \frac{e^{2k(aF - C/F)}}{\omega_k^3} \delta(\omega - \omega_k) \tag{43}$$

or

$$P_1^R(\omega, F) = P_0 \frac{z^2 e^2 \omega_s^2}{2\hbar\omega^3 |\partial\omega_k / \partial k_\omega|} \times e^{2k_\omega (aF - C/F)} \theta(\omega - \omega_s) \theta(\omega_{k_c} - \omega) , \tag{44}$$

where k_ω is implicitly determined by the dispersion relation $\omega = \omega_{k_\omega}$. To fix the ideas, assume a linear dispersion relation (see Fig. 5)

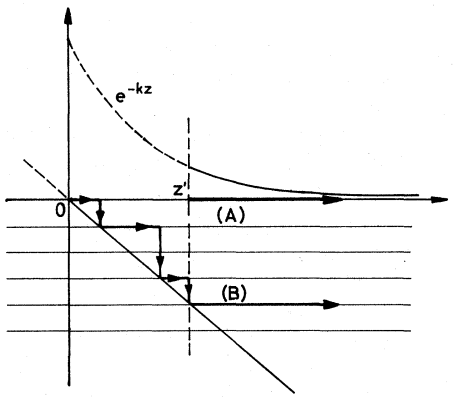

FIG. 4. Illustration of an argument according to which an unscattered ion arriving at z' (case A) is less likely to be scattered in the rest of its flight than an ion which arrives at z' after having already suffered multiple losses (case B).

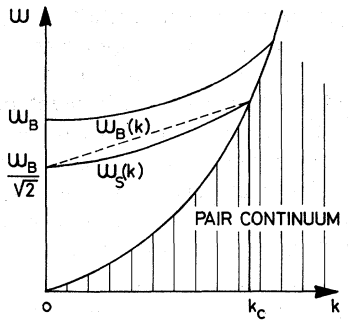

FIG. 5. Energy spectrum of elementary excitations in a semi-infinite free-electron gas (Ref. 14). The bulk plasmon has a parabolic dispersion for small k. The surface plasmon starts with a weak linear k dependence and then picks up the stronger dispersion of the bulk plasmon at larger k. For the transition metals considered above the spectrum of the low-lying collective modes is expected to be a mixture of pure plasmon behavior and pure single-electron interband transitions (Ref. 14). For illustration purposes, a linear surface-plasmon dispersion relation (dashed line) has been used in the text.

$$\omega_k = \omega_s + bk\ , \quad 0 \leq k \leq k_c \tag{45}$$

where b is an *average* dispersion parameter over the whole range $0 \leq k \leq k_c$. This yields

$$P_1^R(\omega, F) = P_0 \frac{Z^2 e^2 \omega_s^2}{2\hbar b \omega^3} \exp\left[2\frac{\omega - \omega_s}{b}\left(aF - \frac{C}{F}\right)\right], \quad \omega_s \leq \omega \leq \omega_{k_c}\ . \tag{46}$$

Thus, according to the sign of the quantity $aF - C/F$, the shape of the single-loss line changes drastically when the field strength passes through the critical value

$$F_c = (C/a)^{1/2}\ . \tag{47}$$

For $F < F_c$, the spectrum is maximum at $\omega = \omega_s$, whereas for $F > F_c$, the maximum will move towards $\omega = \omega_{k_c}$. The actual first-order peak resulting from the multiple folding procedure described in Sec. III will broaden and shift from ω_s at low field to ω_{k_c} at high field (Fig. 6).

Thus the dependence of peak spacing on field strength and also the apparent shrinking of the spacing between deficit peaks of higher order (see Fig. 8 in Ref. 1) can be qualitatively understood as a dispersion-recoil effect. The exact relationship between field and wave vector of those plasmons excited with the highest probability is rather complicated. However, the physical argument is clear; at low fields only long-wavelength surface plasmons have a substantial probability of being excited because only these can generate an electric field beyond the distance where the ion reaches the kinetic-energy threshold $\hbar\omega_k$. Similarly, higher-order loss peaks are generated by losses occurring far away from the tip where only low-k plasmons can reach. Both effects result from the exponential factor e^{-kz} in the interaction Hamiltonian (5). At high fields, on the other hand, recoil effects dominate so that intermediate- or high-k plasmons are also substantially or even predominantly excited.

From Eq. (43), the total integrated intensity of the first-order peak $I_1^R(F)$ divided by the no-loss line intensity $I_0 = P_0$ is found to be

$$\frac{I_1^R(F)}{I_0} = \frac{1}{P_0}\int_0^\infty d\omega\, P_1^R(\omega, F) = \frac{Z^2 e^2 k_c \omega_s^2}{2\hbar\bar{\omega}_s^3}\,\frac{e^{f(F)} - 1}{f(F)}\ , \tag{48}$$

where

$$f(F) = 2k_c(aF - C/F) \tag{49}$$

and the no-loss line intensity itself is

$$I_0 = \exp\left(-\frac{Z^2 e^2 k_c \omega_s^2}{2\hbar\bar{\omega}_s^3}\,\frac{e^f - 1}{f}\right)\ . \tag{50}$$

To obtain Eqs. (48) and (50), we have neglected the dispersion of the denominator in the integrand of Eq. (43) and replaced ω_k by an average value $\bar{\omega}_s \simeq 8.5$ eV over the range $0 \leq k \leq k_c$. For F smaller than F_c, the field function f is negative and one recovers the *linear regime* obtained in Eq. (35),

$$\frac{I_1^R}{I_0} \simeq \frac{-Z^2 e^2 k_c \omega_s^2}{2\hbar\bar{\omega}_s^3}\,\frac{1}{f} \simeq \frac{Z^2 e^2 \omega_s^2}{4\hbar\bar{\omega}_s^3 C}\,F\ , \quad F < F_c\ . \tag{51}$$

For F larger than F_c, f is large and positive and one then finds an *exponential regime*

$$\frac{I_1^R}{I_0} \simeq \frac{Z^2 e^2 k_c \omega_s^2}{2\hbar\bar{\omega}_s^3}\,\frac{e^{2ak_cF}}{2ak_cF}\ , \quad F > F_c\ . \tag{52}$$

An empirical value of the recoil parameter a can be *estimated* by fitting Eq. (48) to the experimentally observed ratio at some field F_c in the transition region from linear to exponential regimes. Applying this rule to the data of Fig. 3 at, say, $F_c \simeq 2.5$ V Å^{-1}, where $I_1/I_0 \simeq 0.2$, yields, from Eqs.

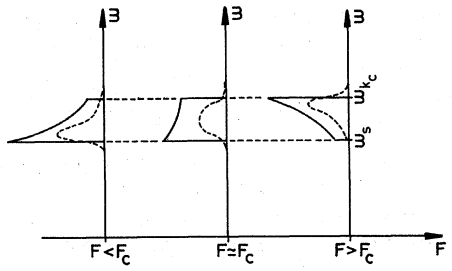

FIG. 6. Theoretical shape of the single-loss line for various field strengths, as predicted by Eq. (46) (full lines). Dashed lines: resulting line shapes when the "bare" lines are folded with a symmetrical instrumental resolution function. The apparent position of the peak of the folded spectrum shifts from ω_s to ω_{k_c} when the field increases above the critical value F_c defined in Eq. (47).

(48) and (49), $a \simeq 1.5\ \mathrm{V^{-1}\,\AA^2}$, in agreement with Eq. (47). To require that the change of regime should take place at a field for which the experimental ratio I_1/I_0 is not too small compared to unity is consistent with the self-generating nature of a recoil event. The recoil enhancement of the loss processes is expected to occur at fields such that the outgoing ions have a substantial chance of recoiling at least once by plasmon emission, i.e., when the probability of being scattered once is comparable to the probability of escaping without loss.

On the basis of the above analysis, the single-loss curve of Fig. 3 may be interpreted as follows. The observed plateau at intermediate fields, on the one hand, would correspond to the linear regime of Eq. (51). The fast exponential increase for fields above $2.7\ \mathrm{V\,\AA^{-1}}$, on the other hand, would be due to recoil enhancement, Eq. (52). If this interpretation is correct, then the initial fast growth of the secondary peak intensities for fields between 1.5 and $2\ \mathrm{V\,\AA^{-1}}$ is not at all understood. However, as pointed out by Jason,[1] this may be a spurious effect of limited instrumental resolution combined with the narrowness of the no-loss line at low fields. Also, the position in Fig. 3 of the crossing points of the successive secondary peak intensities and the detailed shape of these curves are still not accurately predicted by the present semiempirical recoil theory. Obviously, clarification of these fine details requires a more exact quantum theory of recoil and also higher-resolution intensity measurements.

Jason's work provides further experimental evidence in support of our interpretation by the fact that when neon is used as imaging gas, oscillatory distributions are only obtained for fields higher than those necessary in the case of hydrogen (Table I, observation 14). Furthermore, the oscillations are hardly observable when using helium.[13] This can be understood by looking at the respective values of the constant C in Eq. (33) for these three gases. One has[13] $C_{H_2^+} < C_{Ne^+} < C_{He^+}$ and therefore the low-field scattering strength $a \equiv e^2/4z_0\hbar\omega_s = e^2F/4C\hbar\omega_s$ satisfies the condition $a_{H_2^+} > a_{Ne^+} > a_{He^+}$.

VI. PLASMON EFFECTS IN FIELD DESORPTION

The discussion of the problem of plasmon-ion scattering in field evaporation is more involved than in field-ion emission. A first reason is that relatively little is known about the detailed microscopic act of field desorption. In particular, the distance from the surface at which the desorbing atom can be considered as fully ionized is not known. Clearly, from the previous sections, the model parameter z_0 at which the ion is "created" plays an important role since the ion losses are most important near the tip surface. Thus the desorption event and the initial plasmon excitation processes may interfere significantly, whereas in field-ion emission little interference occurs because the characteristic ionization time is much smaller than the acceleration time required by the ion to reach the kinetic-energy threshold $\hbar\omega_s$. A second reason is the very high fields normally used in field evaporation. Evaporation fields of most transition metals[13] fall in the range $4-6\ \mathrm{V\,\AA^{-1}}$, well above the critical field for onset of recoil-enhancement effects in field-ion emission of hydrogen. The crucial question is to determine the regime, either linear or exponential, in which the plasmon excitation by a given evaporating species is taking place. From the results of Sec. V, desorption of hydrogen and light adsorbed species should certainly follow a strong exponential regime since the field function

$$f(F) = 2k_c(aF - z_0) \tag{53}$$

to be used in determining the loss strength of Eq. (48) is positive and large for large F. For desorption of heavier species or for evaporation of metal-tip atoms, however, the situation is not so clear. Recall that the semiclassical recoil parameter a introduced in Eq. (41) is in fact proportional to the ion acceleration $\gamma = ZeF/M$, i.e., to the ion-charge-to-mass ratio. In the limit of very small ratio Z/M, the ion travels so slowly that the metal plasma should be able to readjust the imaging charge adiabatically and hence the inelastic processes should presumably be reduced. Thus for the case of heavy-ion desorption, an estimation of the recoil-enhancement effects is difficult without a better recoil theory. In the rest of this section, we shall therefore confine ourselves to the discussion of light-ion desorption.

Consider a desorption experiment using a field of $4\ \mathrm{V\,\AA^{-1}}$ and whereby an adsorbed hydrogen atom is evaporated from the tip surface and assume that the bare proton emerges at $z_0 \simeq 1$ Å (corresponding to the diameter of the H atom). Using $a \simeq 1$ for the recoil parameter, Eqs. (53), (48), and (20) give, respectively,

$$f \simeq 6\ , \quad I_1^R/I_0 \simeq 50\ , \tag{54}$$

$$P(\tau) = e^{-50} \exp(50\, e^{-t\bar{\omega}_s\tau})\ . \tag{55}$$

According to formula (55), each outgoing ion has practically no chance to leave the tip unscattered. Instead, each one will excite an average number of 50 plasmons, thereby losing 0.4 keV. Some of them may lose up to 100 plasmon quanta. Because of the probabilistic nature of the excitation process, it is impossible to predict how many plasmons any individual preselected atom on the tip surface is going to excite during its flight through the plasmon cloud. What is certain, however, is that if such an atom-probe experiment is repeated a large number

of times, a smooth Poisson-like distribution should emerge with a peak centered roughly at 0.4 keV down from the position of the no-loss line. It should be emphasized that for such an experiment to be statistically meaningful, the number of ions of the expected type collected and analyzed should be orders of magnitude larger than the loss strength $I_1^R/I_0 \simeq 50$ in our example.

What kind of distribution does one expect if more than one family of plasmons (ω_s^μ, k_c^μ) are involved, as seems to be the case for transition metals? For this case, the equation

$$P(\tau) = P_0 \exp\left(\sum_\mu \frac{Z^2 e^2 k_c^\mu (\omega_s^\mu)^2}{2\hbar(\bar{\omega}_s^\mu)^3} \frac{e^{f^\mu(F)} - 1}{f^\mu(F)} \right) \tag{56}$$

must be used. Assume that there are two branches at $\hbar\bar{\omega}_a = 8.5$ eV and $\hbar\bar{\omega}_b = 20$ eV and suppose that the corresponding loss strengths a and b are both approximately equal to 50. Then the loss spectrum

$$P(\omega) = P_0 \int_{-\infty}^{+\infty} d\tau\, e^{i\omega\tau} \exp(a e^{-i\bar{\omega}_a\tau} + b e^{-i\bar{\omega}_b\tau}) \tag{57}$$

$$= P_0 \sum_{m,n} \frac{a^m b^n}{m!\, n!} \delta[\omega - (m\bar{\omega}_a + n\bar{\omega}_b)] \tag{58}$$

has maximum strength for $m = a$ and $n = b$. The distribution will therefore culminate at an energy $\hbar\omega = \hbar(a\bar{\omega}_a + b\bar{\omega}_b) \simeq 1.5$ keV below the expected position of the no-loss line. Also, the width of such a distribution will be of the order of 1 keV, i.e., 10% of the total energy acquired by the proton in a desorbing voltage of, say, 10 keV. Jason's experiments on field *emission* of H_2^+ already give evidence for such wide distributions: "At fields above 3.5 V Å^{-1}, the large tip distributions are hundreds of volts wide and no ions are seen corresponding to the main peak" [Ref. 1, p. 276; see also Figs. 9(d) and 9(f) in this reference].

Statistically unsaturated Poisson-like distributions of evaporated ions have been observed by Müller *et al.*[2] and by Brenner and McKinney.[3] Some of the broad distributions have been interpreted as being due to the transient formation of various molecular ion compounds. As illustrated by the above hydrogen desorption example, an alternative explanation in terms of the present theory is that these distributions may represent single ionic species with energies broadened by the process of multiple plasmon losses. A typical experimental case which could be interpreted along these lines is the broad hydrogen spectrum accompanying the equally broad spectrum of doubly ionized evaporated tantalum ions (Fig. 2 in Ref. 2). Until statistically more significant ion desorption spectra are obtained and until a full quantum-mechanical theory of ion-plasmon multiple scattering is developed, interpretation of the fine structures of field evaporation energy distributions will remain somewhat speculative.

VII. SUMMARY OF CONCLUSIONS

A new theory of the oscillatory ion energy distributions in field-ion emission has been presented. The origin and properties of the secondary peaks have been ascribed to inelastic multiple scatterings of the gas ions by the collective electronic excitations of the metal-tip surface. The previous resonance tunneling theory of the oscillatory distributions does not seem to apply to this physical problem.

The most important consequences of the present interpretation are the following:

(a) The variation of peak spacings with field strength offers a unique way of *mapping* the full dispersion relation of this family of "plasmons" responsible for the ion scattering.

(b) The dependence of the secondary peak intensities on field strength provides additional experimental access to the fundamental parameters of these excitations.

In field desorption, large ion energy losses from the same repeated excitation of the metallic quantum plasma will yield broad energy distributions. Combined with the stochastic nature of plasmon generation, this could result in an irreducible limitation, previously unforeseen, to the mass resolution of the atom-probe microscope as an instrument of single-atom sensitivity.

ACKNOWLEDGMENTS

The author wishes to thank Professor P. Cutler for numerous valuable discussions and for his continued interest in this work. He is also grateful to Dr. R. F. Willis for his critical reading of the manuscript.

---

*Chercheur Qualifié au Fonds National Belge de la Recherche Scientifique.

[1] A. J. Jason, Phys. Rev. 156, 266 (1967).

[2] E. W. Müller, S. V. Krishnaswamy, and S. B. McLane, Surface Sci. 23, 112 (1970).

[3] S. S. Brenner and J. T. McKinney, Surface Sci. 23, 88 (1970).

[4] M. E. Alferieff and C. B. Duke, J. Chem. Phys. 46, 938 (1967).

[5] A preliminary report of this work has appeared in Phys. Rev. Letters 26, 813 (1971).

[6] These physical ideas follow from a normal-mode analysis of Maxwell's equations applied to a semi-infinite solid with dielectric function $\epsilon(\omega)$. See, for instance, A. A. Lucas, E. Kartheuser, and R. Badro, Phys. Rev. B 2, 2488 (1970).

[7] D. W. Juenker, L. J. Le Blanc, and C. R. Martin, J. Opt. Soc. Am. 58, 164 (1968).

[8]K. A. Kress and G. J. Lapeyre, J. Opt. Soc. Am. 60, 1681 (1970).

[9]R. F. Willis (private communication).

[10]A. A. Lucas and M. Šunjić, Phys. Rev. Letters 26, 229 (1971).

[11]M. Šunjić and A. A. Lucas, Phys. Rev. B 3, 719 (1971).

[12]A. A. Lucas and M. Šunjić, Progr. Surface Sci. (to be published).

[13]E. W. Müller and Tien Tsou Tsong, *Field Ion Microscopy* (Elsevier, New York, 1969).

[14]D. Pines, *Elementary Excitations in Solids* (Benjamin, New York, 1964).

[15]A. Messiah, *Quantum Mechanics* (North-Holland, Amsterdam, 1970).

[16]*Handbook of Mathematical Functions*, edited by M. Abramovitz and I. A. Stegun (U. S. GPC, Washington, D. C., 1965).